JACS
JOURNAL OF THE AMERICAN CHEMICAL SOCIETY

ARTICLE

pubs.acs.org/JACS

Mechanistic Investigations of Cooperative Catalysis in the Enantioselective Fluorination of Epoxides

Julia A. Kalow and Abigail G. Doyle*

Department of Chemistry, Princeton University, Princeton, New Jersey 08544, United States

Supporting Information

ABSTRACT: This report describes mechanistic studies of the (salen)Co- and amine-cocatalyzed enantioselective ring opening of epoxides by fluoride. The kinetics of the reaction, as determined by in situ ^{19}F NMR analysis, are characterized by apparent first-order dependence on (salen)Co. Substituent effects, nonlinear effects, and reactivity with a linked (salen)Co catalyst provide evidence for a rate-limiting, bimetallic ring-opening step. To account for these divergent data, we propose a mechanism wherein the active nucleophilic fluorine species is a cobalt fluoride that forms a resting-state dimer. Axial ligation of the amine cocatalyst to (salen)Co facilitates dimer dissociation and is the origin of the observed cooperativity. On the basis of these studies, we show that significant improvements in the rates, turnover numbers, and substrate scope of the fluoride ring-opening reactions can be realized through the use of a linked salen framework. Application of this catalyst system to a rapid (5 min) fluorination to generate the unlabeled analog of a known PET tracer, F-MISO, is reported.

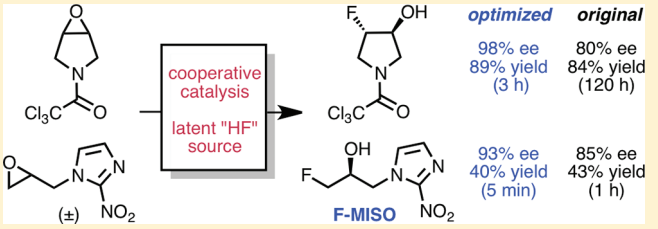

INTRODUCTION

Fluorinated organic molecules display broad utility as valuable pharmaceuticals, radiotracers, performance materials, and agrochemicals.[1] With its high electronegativity and small van der Waals radius, fluorine influences molecular conformation, the pK_a of neighboring heteroatoms, and reactivity.[2] In biologically active targets, C−F bonds are incorporated into organic molecules to modulate useful physical properties, including lipophilicity, bioavailability, and oxidative stability. Despite the widespread utility of fluoroorganics, chemists are often limited to commercially available fluoroarenes and perfluoroalkanes for chemical synthesis due to the harsh conditions required in established fluorination methods and the scarcity of naturally occurring organofluorine compounds.[3] Furthermore, there exist few strategies for the late-stage incorporation of fluorine that can be applied to the synthesis of novel ^{18}F-labeled tracers for positron emission tomography (PET).[4]

As such, catalytic carbon−fluorine bond formation has emerged as a highly desirable but challenging approach to the synthesis of fluorine-containing targets. New methods for the formation of aliphatic C−F bonds have the potential to deliver useful chiral fluorinated structures inaccessible from commercial or biogenic sources. In this regard, the most significant advances have relied upon the use of electrophilic "F$^+$" equivalents.[5] A variety of chiral Lewis acids and organocatalysts have been identified that enable highly enantioselective α-fluorination of carbonyl-containing compounds with these reagents. However, electrophilic fluorine sources suffer from high cost and, in PET applications, low specific activity. The use of abundant, inexpensive nucleophilic fluorine sources, such as metal fluorides or HF-containing reagents, has the potential to deliver complementary fluorinated building blocks and to access mechanisms amenable to radiosynthesis. Unfortunately, previous efforts to effect catalysis of nucleophilic fluorination through manifolds well precedented for other nucleophiles have been hindered by fluoride's high electronegativity and low polarizability, which make it a recalcitrant nucleophile and relatively strong base in organic solvents.[6]

In 2010, our group disclosed the first catalytic, highly enantioselective methods for nucleophilic fluorination of epoxides[7] and allylic chlorides.[8] Bruns and Haufe had previously reported investigations of fluoride ring opening of epoxides in the presence of stoichiometric chiral (salen)M complex **1**·Cl (Figure 1).[9] Their work established that the use of silver fluoride as a fluorinating reagent could afford products in up to 74% ee. However, catalytic turnover of **1** could not be achieved, and elevated temperatures were required for fluorohydrin formation, presumably due to the low solubility of AgF in the reaction media. The authors also found that use of a variety of other nucleophilic fluorine sources led to either no reaction (e.g., $Et_3N \cdot 3HF$) or no asymmetric induction (e.g., Olah's reagent, HF-pyridine[10]) due to facile catalyst poisoning or background activity. Instead, we discovered that use of benzoyl fluoride and 1,1,1,3,3,3-hexafluoroisopropanol (HFIP) as a latent source of HF provided access to an organic-soluble fluorinating reagent in a manner compatible with asymmetric catalysis. We reported that chiral Lewis acid (*R*,*R*)-**2** promoted highly enantioselective fluoride ring opening

Received: April 18, 2011
Published: August 24, 2011

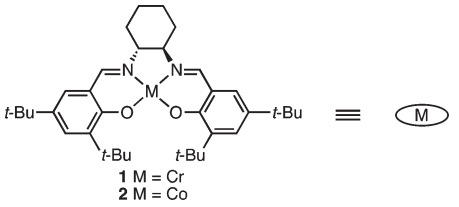

Figure 1. (Salen)Co catalysts used in ring-opening reactions.

Table 1. Lewis Acid–Amine Cooperative Catalysis

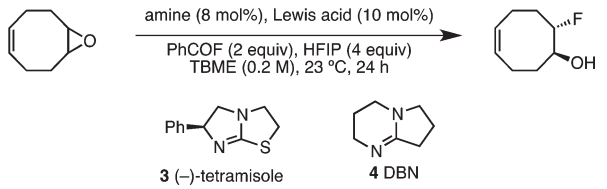

entry	amine	Lewis acid	conv. (%)[a]	ee (%)[b]
1	none	(*R*,*R*)-**2**	17	55
2	(−)-**3**	(*R*,*R*)-**2**	88	95
3	(−)-**3**	(*S*,*S*)-**2**	8	−32
4[c]	**4**	(*R*,*R*)-**2**	25	53

[a] Determined by GC using 1-decene as a quantitative internal standard. [b] Determined by chiral GC analysis using commercial chiral columns. [c] Average data for two experiments.

in combination with this novel, latent HF source and an amine cocatalyst. In the desymmetrization of meso epoxides, chiral isothiourea cocatalyst (−)-tetramisole ((−)-**3**) afforded highest selectivities. Notably, a significant matched-mismatched effect on both yield *and* enantioselectivity was observed between **2** and **3** (Table 1, entries 2 and 3). For the kinetic resolution of terminal epoxides, which is selective for ring opening at the least substituted position, we found instead that the achiral amidine 1, 5-diazabicyclo[4.3.0]non-5-ene (DBN, **4**) was optimal. Such intriguing cooperative behavior has little precedence in Lewis acid–amine cocatalysis. While the cocatalytic reactions are characterized by remarkably mild and selective conditions for nucleophilic fluorination, in certain cases high catalyst loadings and extended reaction times were required. As such, the low reaction rates precluded applications for the radiosynthesis of PET tracers (the half-life of the radioisotope ^{18}F is 110 min). To achieve synthetic improvements, and to elucidate the role of the amine cocatalyst, we engaged in mechanistic investigations of the ring-opening reaction.

Jacobsen and co-workers have extensively studied the mechanism of ring openings catalyzed by **1** and **2**[11] for the desymmetrization of meso epoxides by azide[12] and the hydrolytic kinetic resolution (HKR) of terminal epoxides.[13] Kinetic studies have shown that both reactions are second order in catalyst in the rate-limiting step; moreover, a nonlinear relationship between the ee of ring-opened product and the ee of the catalyst has implicated two (salen)M molecules in the enantiodetermining step. On the basis of these data, a consensus mechanism has been proposed, which involves one (salen)M center activating the epoxide and another delivering the nucleophile in a homobimetallic pathway (Scheme 1).

Herein, we describe mechanistic investigations aimed at elucidating the roles of **2**–**4** in the cocatalytic ring opening of meso and terminal epoxides by fluoride anion. The mechanism of the kinetic resolution, which proved more amenable to analysis, was evaluated in detail. Kinetic studies revealed an apparent first-order dependence on [**2**]; in contrast, experiments probing substituent effects, nonlinear effects, and reaction rates with a linked catalyst establish bimetallic ring opening as the rate-limiting step. These data are reconciled by the occurrence of a resting-state dimer, and a combination of techniques allows us to propose a catalytic cycle involving (salen)CoF(HF) as the active fluorinating agent. The unique reactivity and selectivity of this species, and the origin of cooperativity between (salen)Co and amine, appear to be derived from axial ligation of the amine cocatalysts to the cobalt center. Finally, we report that the use of linked (salen)Co catalysts[14] provides significant synthetic improvements in terms of rate, catalyst loading, enantioselectivity, and substrate scope.

Scheme 1. A Bimetallic Mechanism Accounts for High Selectivity in Ring-Opening Reactions

RESULTS AND DISCUSSION

Kinetic Studies. To shed light on the mechanism of cooperativity between **2** and cocatalysts (−)-**3** and **4**, we initated kinetic studies using the ring opening of terminal epoxides as a representative cocatalytic reaction. Blackmond's reaction progress kinetic analysis[15] was performed with 4-fluorostyrene oxide (**5**) as a model substrate, which undergoes kinetic resolution with a selectivity factor (*s*) of >100. Using in situ ^{19}F NMR and 1, 4-difluorobenzene as a quantitative internal standard, the entire course of the reaction was monitored under synthetically relevant conditions. Conveniently, the conversions of **5**, benzoyl fluoride, and HFIP could be quantified, along with the formation of the fluorohydrin **6** and 1,1,1,3,3,3-hexafluoroisopropyl benzoate (**7**), the byproduct derived from solvolysis of benzoyl fluoride by HFIP (eq 1).[16] To simplify the kinetics, only the matched enantiomer (*R*)-**5** was used in combination with (*S*,*S*)-**2**.

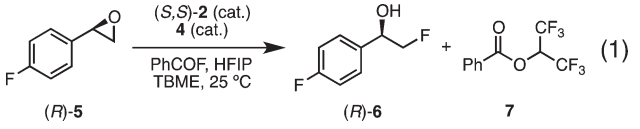

(1)

The raw NMR data for a typical reaction are shown in Figure 2, and the corresponding concentration versus time data are shown in Figure 3A. Notably, the reaction proceeds cleanly, without any observable fluorinated side products, and the sum of the concentrations of **5** and **6** remains constant over the course of the reaction. Furthermore, the generation of ester **7** occurs at approximately the same rate as that of **6** until the epoxide is fully consumed, implying that minimal unproductive reaction of HF with the glass reaction vessel occurs.

Through differentiation, the concentration versus time data may be processed to provide a plot of rate (−d[**5**]/d*t*) versus [**5**] (Figure 3B).[15] On the basis of parallel UV–vis/rate measurements, we established that aerobic oxidation of the Co(II)

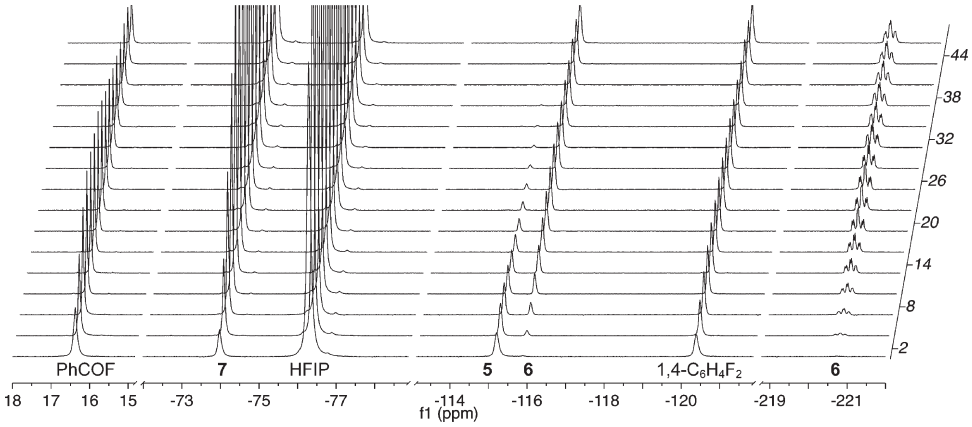

Figure 2. Representative ^{19}F NMR data for the reaction shown in eq 1: [**2**] = 10 mM, [**4**] = 8 mM, [**5**]$_0$ = 227 mM, [PhCOF]$_0$ = 444 mM, [HFIP]$_0$ = 475 mM, [1,4-$C_6H_4F_2$] = 100 mM.

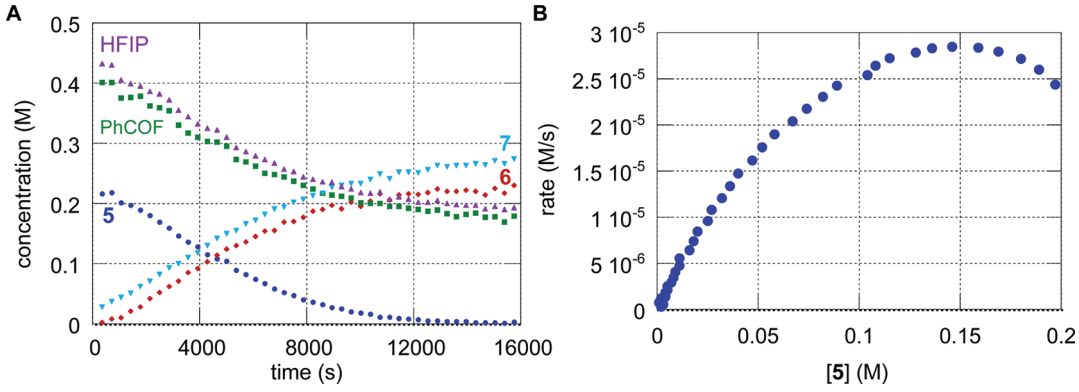

Figure 3. (A) Concentration vs time for the data shown in Figure 2, and (B) rate (−d[**5**]/dt) vs [**5**].

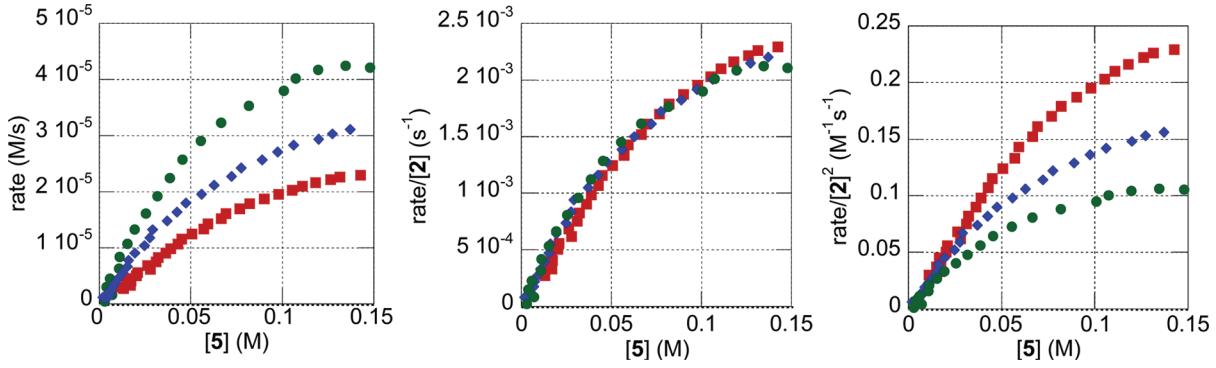

Figure 4. Graphical rate equations for 0th-, 1st-, and 2nd-order dependence on [**2**] for 10 mM (red squares), 14.1 mM (blue diamonds), and 20 mM (green circles) **2** (eq 1, [**4**] = 8 mM, [**5**]$_0$ = 220 ± 7 mM, [PhCOF]$_0$ = 436 ± 12 mM, [HFIP]$_0$ = 455 ± 20 mM, [1,4-$C_6H_4F_2$] = 100 mM).

precatalyst **2** to the active Co(III) species is responsible for the induction period during the early stages of the reaction, as is seen in Figure 3B.[17] Since preoxidized catalysts were found to be less effective than **2** and the rate of oxidation was dependent on the ratio of **2** to cocatalyst **4**, we have omitted the induction period from analysis of the graphical rate equations in subsequent plots.

The order of **2** in the ring-opening reaction was determined by comparing reaction rates at 10, 14.1, and 20 mM **2**, while keeping constant the initial concentrations of all other reactants. Omitting the induction period, overlay of the data is seen in the graphical rate equation corresponding to first-order dependence on [**2**] (Figure 4). Significantly, this kinetic dependence on **2** is distinct from that of ring-opening reactions with other nucleophiles, which are second order in (salen)M, and warranted further study.

Investigation of the kinetic role of the amidine cocatalyst was conducted in a similar manner. Graphical rate equations for reactions using 4 and 8 mM **4** indicate that the reaction is first order in amidine (Figure 5). Furthermore, graphical rate equations for reactions run with the same catalyst concentrations and different starting points ("same excess" experiments[15]) showed

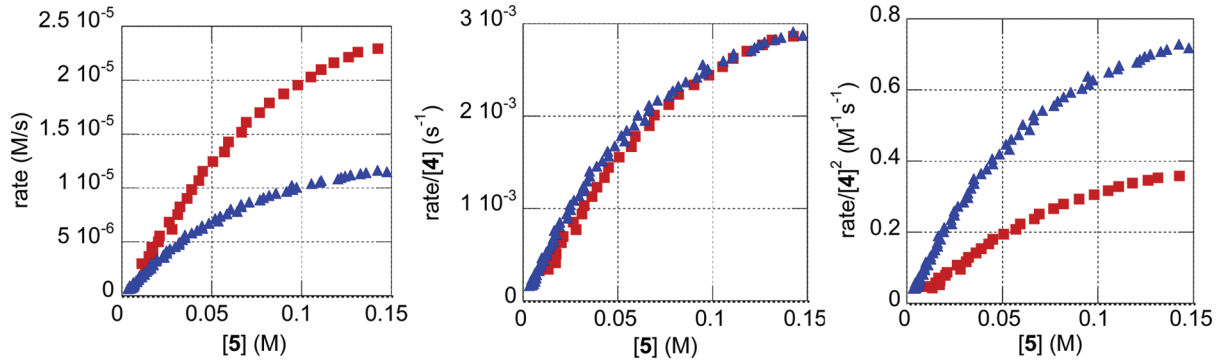

Figure 5. Graphical rate equations for 0th-, 1st-, and 2nd-order dependence on [**4**] with 4 mM (blue triangles) and 8 mM (red squares) **4** (eq 1, [**2**] = 10 mM, $[\mathbf{5}]_0$ = 224 ± 10 mM, $[PhCOF]_0$ = 438 ± 6 mM, $[HFIP]_0$ = 542 ± 131 mM, [1,4-$C_6H_4F_2$] = 100 mM).

overlay, confirming that the catalysts do not experience decomposition over the course of the reaction, and that neither product inhibition nor autocatalysis is operative.[18]

To explain the discrepancy between the observed first-order dependence on [**2**] in the fluorination reactions and the second-order behavior previously reported for ring-opening reactions with other nucleophiles, we have considered three possible scenarios:

(a) Ring-opening is not the rate-limiting step.
(b) Ring-opening is rate limiting and involves one (salen)Co species.
(c) Ring-opening is rate limiting and involves two (salen)Co species; the apparent first-order dependence on [**2**] arises from a resting-state dimer.

Initial rate data for fluorinations conducted with varying concentrations of epoxide **5** showed a positive-order dependence on [**5**] at synthetically relevant concentrations (0.1−0.3 M) and saturation at high initial concentrations, indicative of a pre-equilibrium between catalyst and **5**. Consistent with this proposal, the presence of mismatched epoxide (*R*)-**5** inhibited the reaction. At 0.2 M $[\mathbf{5}]_0$, saturation kinetics in benzoyl fluoride were observed; this appears to be the source of the nonlinearity observed in the graphical rate equations (e.g., Figure 3B).[19] Measuring the dependence of initial rate on [HFIP] revealed a more complicated relationship. In particular, a zeroth-order dependence on [HFIP] was observed at synthetically relevant concentrations (0.15−0.4 M), but higher concentrations of HFIP resulted in rate inhibition. Inhibition could arise from a medium effect, as it was found that HFIP is not a competent solvent for the fluorinations.[20] Since the three scenarios described above could not be distinguished by these data, we turned to alternative physical organic experiments to probe the reaction mechanism.

Substituent Effects. A Hammett study was conducted to distinguish between scenarios (a) and (b) or (c) by assessing the impact of electronic variation at the epoxide on reaction rate. The use of Hammett correlations is a well-established technique to provide information about the rate-limiting step.[21] Accordingly, a series of *para*-substitued styrene oxides were subjected to competition experiments with styrene oxide under optimized conditions (eq 2).[22] In the competition experiments, the ratio of conversions at an early time point (<20% total conversion) was used to approximate k_X/k_H. We found that the Hammett constants σ_m provided the best linear correlation with $\log(k_X/k_H)$ (R^2 = 0.97), suggesting that there is little resonance contribution to the rate differences between substituted epoxides (Figure 6).[23,24] Notably, a large positive ρ value, +1.98 ± 0.19, was obtained.

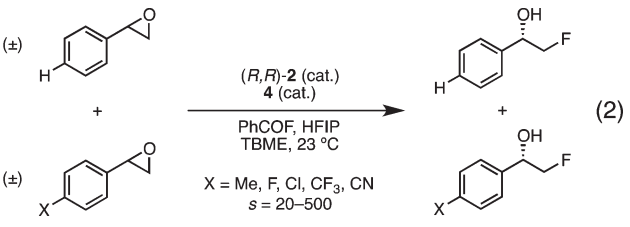

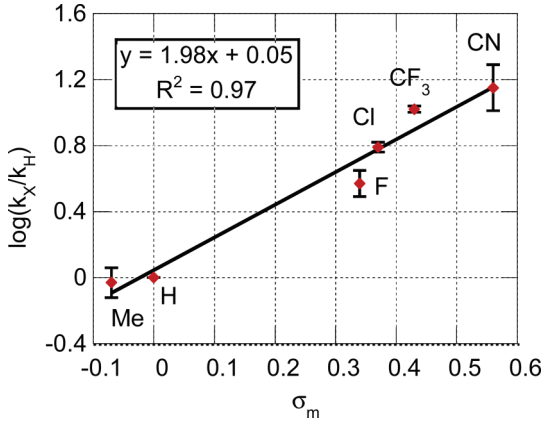

Figure 6. A Hammett plot for the catalytic ring opening of *para*-substituted styrene oxides by fluoride (eq 2). Each data point represents the average of two or three experiments; error bars are standard deviations.

This value, which indicates that the transition state experiences negative charge buildup, is consistent with rate-limiting ring opening. Indeed, previous reports on terminal opening of *para*-substitued styrene oxides under enzymatic[25] and basic[26] catalysis have described ρ values ranging from +0.3 to +0.87. For the fluorination reaction, the magnitude of the observed ρ value could indicate a later transition state. Alternatively, if the rate-limiting step were not associated with ring-opening (scenario (a)), the positive-order kinetic dependence on [epoxide] would be best explained by the epoxide serving as a neutral axial ligand to **2**. Since electron-rich epoxides are expected to be more effective ligands for a Lewis acid, the corresponding ρ value would be small and negative, inconsistent with the experimental data. Given these considerations, the data are most consistent with scenarios (b) and (c).

Nonlinear Effects. Having established that ring opening is rate limiting on the basis of a positive Hammett correlation,

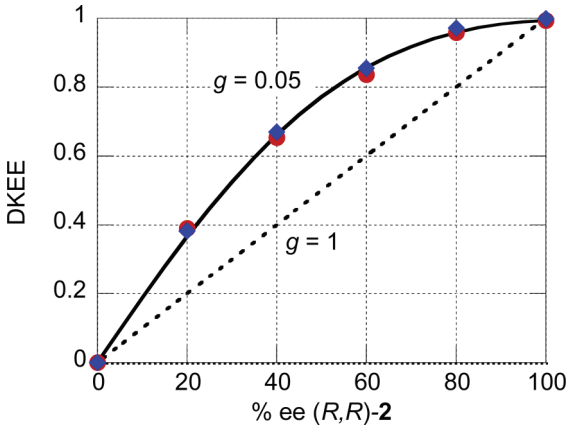

Figure 7. Nonlinear effects in the kinetic resolution of styrene oxide (red circles) and hexene oxide (blue diamonds) (5 mol % **2**, 4 mol % **4**, 2 equiv PhCOF, 2 equiv HFIP, 0.2 M in TBME, 23 °C), and simulations of Kagan's ML_2 model (solid line, $K = 4$, $g = 0.05$, $DKEE_0 = 0.995$) and a linear model (dashed line, $g = 1$). Each data point represents the average of two experiments.

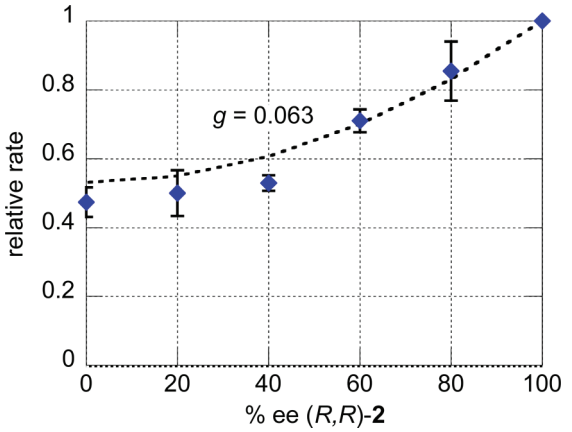

Figure 8. Influence of catalyst ee on initial rate (blue diamonds) in the kinetic resolution of styrene oxide (5 mol % **2**, 4 mol % **4**, 2 equiv PhCOF, 2 equiv HFIP, 0.2 M in TBME, 23 °C), and a simulation of Kagan's ML_2 model (dashed line, $K = 4$, $g = 0.063$). Each data point represents the average of three experiments; error bars are standard deviations.

we turned to nonlinear effects as a further mechanistic probe of this step, which is by definition enantiodetermining.[27] We anticipated that these nonlinear effects studies would inform the possibilities that ring-opening follows a monometallic pathway (b) or that ring opening proceeds by a bimetallic pathway (c).

Johnson and Singleton have shown that the quantity $(s - 1)/(s + 1)$, termed dynamic kinetic enantiomeric enhancement (DKEE), is linearly related to ee_{cat} for monomeric, noninteracting catalysts in kinetic resolutions.[28] For the kinetic resolutions of 1-hexene oxide and styrene oxide by fluoride ring opening, however, we found that the relationship between DKEE and ee_{cat} displayed a pronounced positive nonlinear effect (Figure 7). Nevertheless, kinetic resolutions can exhibit nonlinear effects in the *absence* of interacting catalysts if kinetic partitioning occurs: that is, if the chiral catalyst binds to each enantiomer of substrate with different affinities.[29] Kinetic partitioning can offer an alternative explanation for nonlinear effects, or it can magnify nonlinear effects derived from catalyst interaction. To determine the degree of kinetic partitioning in the cocatalytic fluorination, we measured the normalized selectivity factor s at different substrate conversions for the reaction of 1-hexene oxide using scalemic catalyst. For highly selective kinetic resolutions ($s > 100$) subject to kinetic partitioning, modeling indicates that s should increase dramatically at high conversions; significant variation was not observed for fluoride ring opening, suggesting that kinetic partitioning provides a minor contribution to enantiodifferentiation, if any (see Supporting Information, Figure S19). Therefore, the significant nonlinear effects depicted in Figure 7 may be ascribed to interaction between the chiral (salen)Co species.

In addition, a kinetic dependence on the ee of the catalyst was observed.[30] Relative rates for the kinetic resolution of styrene oxide using 0−100% ee (*R*,*R*)-**2** were measured and rate suppression was found (Figure 8).[31] Since these data are initial rates, contributions from kinetic partitioning (if relevant) are negligible. Notably, these rate data also support the conclusion from the Hammett studies that ring opening is the rate- as well as the enantiodetermining step.

For reactions displaying nonlinear effects, Kagan has derived models that can be used to elucidate the number of interacting chiral species and the nature of their interactions.[32] We compared Kagan's ML_2 model, which predicts $ee_{product}$ for two interacting chiral species, to the data in Figures 7 and 8 using the parameter DKEE in place of $ee_{product}$. According to this model, for a statistical distribution of chiral species ($K = 4$), DKEE can be predicted by eq 3, in which $DKEE_0$ is the experimental value using enantiopure catalyst, and g is the relative rates of the heterochiral and homochiral pathways. This model was in excellent agreement with the nonlinear effect data and kinetic dependence on scalemic **2** for $g = 0.053$ (1-hexene oxide) and 0.063 (styrene oxide).[33] Although Kagan's ML_2 model is typically applied to ground-state complexes, if one considers that the noncovalent approach of any two molecules of **2**·epoxide and **2**·Nu in the transition state is statistically determined, eq 3 should apply even if the physical meaning of K is different.[34]

$$DKEE = DKEE_0 ee_{cat} \frac{2}{1 + g + (1 - g)ee_{cat}^2} \quad (3)$$

The nonlinear effects on reaction selectivity and rate provide conclusive evidence for interaction between two (salen)Co species and the fit to Kagan's ML_2 model is consistent with cooperative bimetallic ring opening. However, the data do not distinguish between this mechanism and a reservoir effect,[35] wherein the minor enantiomer of catalyst is sequestered in inactive heterochiral dimers. A bimetallic rate-limiting step favoring the homochiral combination of catalysts is consistent with previous mechanistic studies of (salen)M-catalyzed epoxide-opening reactions, but appears to be inconsistent with the first-order kinetic dependence on [**2**]. The reservoir effect is compatible with the kinetic data, but would require a ring-opening step that diverges from the established model for (salen)M catalysts.[36] Thus, further experiments were performed to distinguish between mechanisms (b) and (c).

Dimeric Catalysts As a Mechanistic Probe. To interrogate the possibility of cooperative bimetallic ring opening, we conducted mechanistic experiments with dimeric catalyst (*R*,*R*,*R*,*R*)-**8** (Figure 9). Catalyst **8** has been shown to enhance cooperative reactivity in the cyclization of epoxy alcohols and in the copolymerization of epoxides and CO_2.[37] Catalyst (*R*,*R*,*R*,*R*)-**8**, when oxidized in situ to an active Co(III) species by equimolar

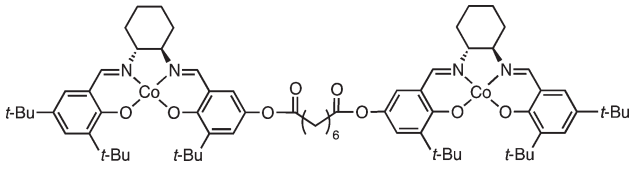

Figure 9. (*R*,*R*,*R*,*R*)-**8**.

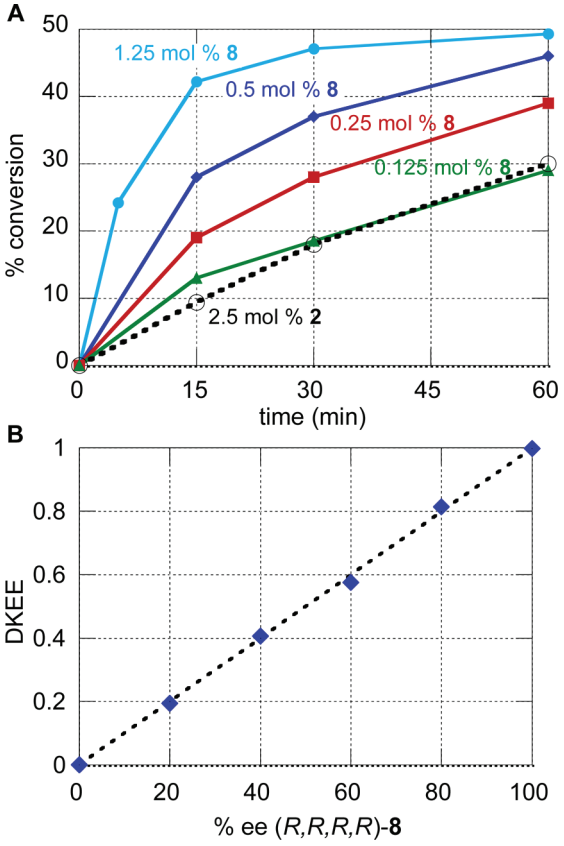

Figure 10. (A) Rate acceleration in the kinetic resolution of hexene oxide using 1.25 (light blue circles), 0.5 (blue diamonds), 0.25 (red squares), and 0.125 (green triangles) mol % dimeric catalyst (*R*,*R*,*R*,*R*)-**8** compared to 2.5 mol % (*R*,*R*)-**2** (open circles) (0.8 equiv **4** relative to Co, 1 equiv *t*-BuOOH relative to Co, 0.55 equiv PhCOF, 0.825 equiv HFIP, 0.4 M in TBME, 24 °C). (B) DKEE (blue diamonds) vs % ee **8** with 1 mM **8** in the kinetic resolution of hexene oxide and a linear model (dashed line).

t-BuOOH,[38] provided approximately 10-fold rate acceleration in the ring opening of hexene oxide compared to the reaction catalyzed by (*R*,*R*)-**2** (Figure 10A).[39] In addition, nonlinear effects were *not* observed when 0.25 mol % scalemic **8**, prepared from mixtures of (*R*,*R*,*R*,*R*)- and (*S*,*S*,*S*,*S*)-**8**, was used in the kinetic resolution of hexene oxide. The strictly linear relationship between DKEE and % ee **8** ($R^2 > 0.99$, Figure 10B) implies that productive intermolecular interactions between salen units do not occur under these conditions.

Taken together, these data provide substantial evidence for a bimetallic ring-opening step, in accordance with existing mechanistic models for (salen)M-catalyzed ring opening (Scheme 1). However, such a scenario would be expected to exhibit a second-order kinetic dependence on [**2**] and first-order dependence on [**8**]. Notably, kinetic analysis of the reaction of (±)-hexene oxide catalyzed by 0.125 and 0.25 mol % (*R*,*R*,*R*,*R*)-**8**, as

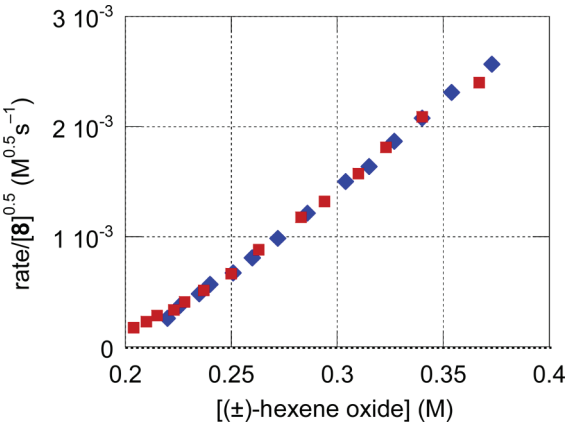

Figure 11. Graphical rate equation for half-order dependence on [**8**] in the kinetic resolution of hexene oxide for 0.5 (blue diamonds) and 1 (red squares) mM **8**; each data point represents the average of three experiments. The reactions were monitored by GC using 1-decene as a quantitative internal standard (0.8 mM **4**, 1 equiv *t*-BuOOH relative to Co, 0.55 equiv PhCOF, 0.825 equiv HFIP, 0.4 M in TBME, 24 °C). See Supporting Information for graphical rate equations for 0th- and 1st-order dependence on [**8**].

Scheme 2. Effect of a Resting-State Dimer on Kinetics

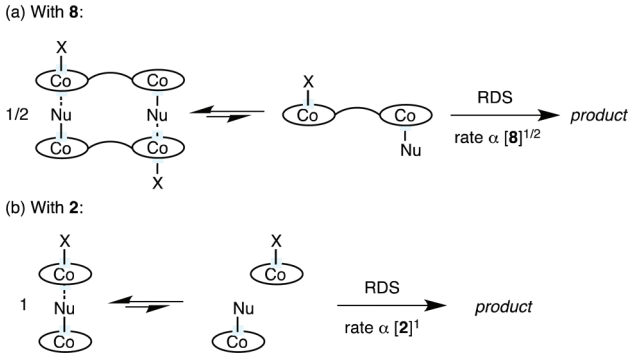

monitored by GC to at least 90% conversion of the matched enantiomer, revealed a *half*-order depenedence on [**8**] (Figure 11).[40] In catalytic reactions, such half-order kinetics are the hallmark of an inactive resting-state dimer (Scheme 2a).[41] Significantly, the absence of nonlinear effects with **8** reveals that differential formation of the hetero- or homochiral resting-state dimers does not occur: such a reservoir effect would result in asymmetric amplification or depletion. Additionally, intramolecular deactivation of the cobalt centers in **8**, which would prevent the rate acceleration observed in Figure 10A, is presumably disfavored by constraints imposed by the dicarboxylate tether.

Similarly, the formation of an analogous resting-state dimer in the **2**-catalyzed reaction, which must dissociate prior to a bimetallic rate-limiting step, provides an explanation for the unusual apparent first-order dependence on [**2**] (Scheme 2b, scenario (c)). In other words, since the molecularity of the resting state and the transition state are the same with respect to **2**, first-order kinetics are observed. To the best of our knowledge, this precise scenario has not been described previously.[42]

The unique tendency of the active (salen)Co(III) species in the fluoride ring-opening reaction to exist preferentially as a dimer is best attributed to a bridging fluoride or bifluoride

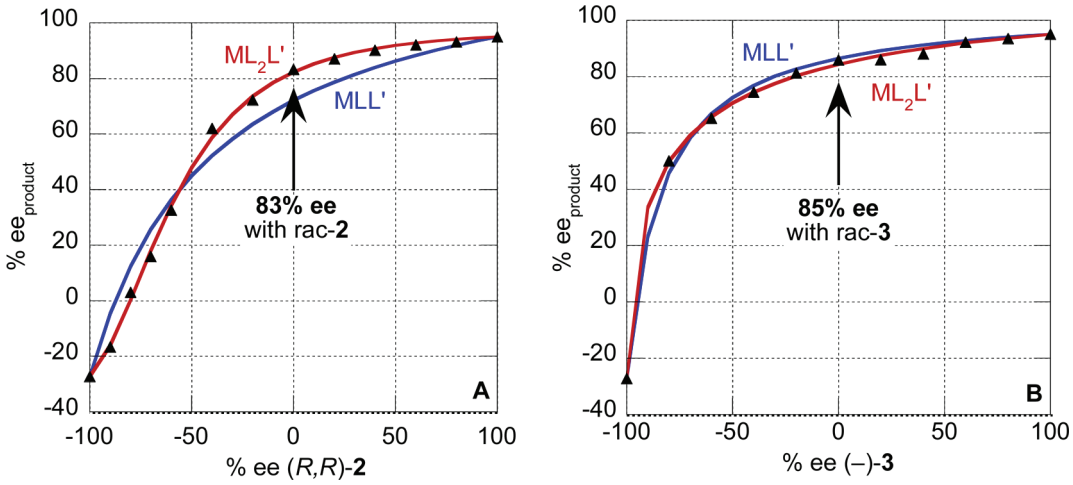

Figure 12. Nonlinear effects in the desymmetrization of cyclooctadiene monoxide (▲) using (A) scalemic **2** and (B) scalemic **3** (10 mol % **2**, 8 mol % **3**, 2 equiv PhCOF, 4 equiv HFIP, 0.2 M in TBME, 23 °C, 18 h; $EE_{mat} = 95.0$, $EE_{mis} = -27.3$), and simulations of MLL′ (blue line, $\alpha_A = 0.230$; $\alpha_B = 0.075$) and ML_2L' (red line, $\beta_A = 0.141$, $\gamma_A = 0.068$, $EE_{mix,A} = 45.5$; $\beta_B = 0.254$, $\gamma_A = 0.005$, $EE_{mix,A} = 44.5$).

complex. Both dimeric and polymeric fluoride- and bifluoride-bridged transition-metal complexes have been characterized.[43] Additionally, the tendency of (salen)M species to oligomerize in the presence of counterions such as azide and methoxide has been reported.[44,12a] Unfortunately, NMR spectroscopic studies have not led to successful characterization of such monomeric or dimeric Co(III)−F species due to the paramagnetic Co(III) center.[45] While we have generated (salen)Co(III) complexes that are stoichiometrically active for enantioselective ring opening in the absence of exogeneous fluoride, these species are highly soluble in organic solvents, including pentane, and various methods for recrystallization have not yet yielded X-ray-quality crystals (see Supporting Information for details). Nevertheless, the mechanistic data and the reactivity of the nucleophilic fluorine source are best explained by the intermediacy of a cobalt fluoride.

Lewis Acid−Amine Cooperative Catalysis. Sequestration of the catalyst in an inactive dimeric resting state provides an explanation for the sluggishness of the ring-opening reaction beyond the inherently poor nucleophilicty of fluoride. Since Lewis basic additives are known to disrupt (salen)M oligomers,[46] the rate acceleration conferred by the amidine or isothiourea cocatalyst could be attributed in part to its role in increasing the concentration of active monomeric catalyst. Accordingly, spectroscopic data for kinetically competent (salen)Co species in combination with (−)-**3** and **4** were consistent with binding.[47] Specifically, FTIR reveals a shift in $\nu_{C=N}$ for amidine **4** in the presence of (salen)Co(III), and the UV−vis absorption at ca. 800 nm characteristic of five-coordinate (salen)Co(III) complexes decreases upon addition of **3** or **4** (see Supporting Information for details).[48] Moreover, kinetic experiments established a role for **4** in or prior to the rate-limiting step. To evaluate the interaction between (salen)Co and the isothiourea cocatalyst **3** in more detail, we turned to nonlinear effect studies in the desymmetrization reactions.

The significant matched-mismatched effect observed between **2** and (−)-**3**, which affects both rate and enantioselectivity, provides evidence for a cooperative interaction between the two catalysts in the ring-opening step (Table 1).[49] While many models have been developed to describe nonlinear effects in reactions with only one chiral catalyst or auxiliary, analogous models for reactions featuring two distinct chiral catalysts are not found in the literature.[50]

Experimentally, we probed the stoichiometry of each catalyst in the enantiodetermining step by varying its ee while using enantiopure cocatalyst. It is important to note that in the presence of two distinct interacting chiral catalysts, nonlinear effects on the ee of product will be observed even if the enantiodetermining step is first order in each catalyst. We therefore derived equations for first-order (MLL′, eq 4) and second-order (ML_2L', eq 5) dependence on the scalemic catalyst (see Supporting Information for derivation and definitions of variables). Like Kagan's models for nonlinear effects, these use experimental data for product ee in the matched and mismatched cases (EE_{mat} and EE_{mis}), and rely on mathematical modeling to assign the parameters α, β, γ and EE_{mix}. The number of adjustable parameters in eq 5 that are not determined experimentally remains a limitation of these models.

$$ee_{prod} = \frac{[L_R]EE_{mat} + \alpha[L_S]EE_{mis}}{[L_R] + \alpha[L_S]} \quad (4)$$

$$ee_{prod} = \frac{[L_R]^2EE_{mat} + \beta[L_S]^2EE_{mis} + \gamma[L_R][L_S]EE_{mix}}{[L_R]^2 + \beta[L_S]^2 + \gamma[L_R][L_S]} \quad (5)$$

Nevertheless, in the ring opening of cyclooctadiene monoxide with scalemic **2** and enantiopure isothiourea (−)-**3** under standard conditions (see Table 1), the enantiodetermining step was found to unambiguously involve two (salen)Co species, consistent with bimetallic ring opening (Figure 12A). For the nonlinear effects with enantiopure **2** and scalemic **3**, however, scenarios with one or two isothioureas in the enantiodetermining step could not be distinguished on the basis of eq 4 and 5 alone (Figure 12B). Kinetic data for the ring opening of terminal epoxides, as well as the observation that excess isothiourea cocatalyst relative to **2** lowers enantioselectivity, suggest that there is only one isothiourea cocatalyst involved in the ring-opening step.

The pronounced nonlinear effects observed in Figure 12 can prove synthetically useful: the use of racemic **2** or racemic **3** in the presence of enantiopure cocatalyst provided product in 83 and 85% ee, respectively. Thus, cooperative catalysis with two chiral

Scheme 3. Proposed Mechanism

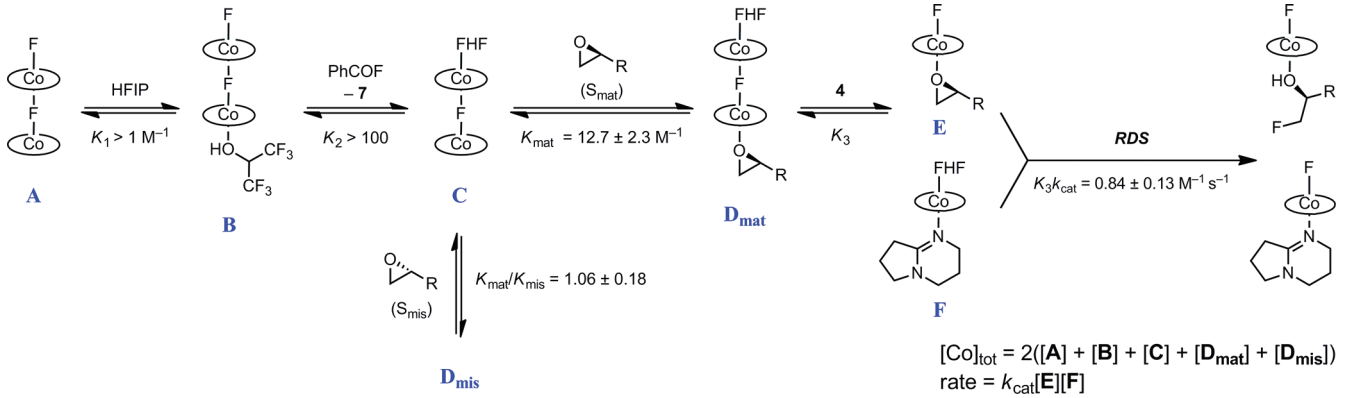

catalysts may prove an effective strategy for optimization even if only one catalyst is available in enantiopure form.

The nonlinear effects studies described above established that the (−)-**3**-cocatalyzed fluoride ring opening of meso epoxides involves two (salen)Co species, consistent with the mechanistic studies of the kinetic resolution. Given this mechanistic congruence, it is striking that amidine **4**, while effective in the kinetic resolution, provided significantly depressed rates and ee's in the desymmetrization relative to chiral isothiourea (−)-**3** (Table 1, entry 4). To better understand the requirement for "tuning" the amine cocatalyst to the electrophile, we evaluated nonlinear effects for the **4**-cocatalyzed desymmetrization. When **4** was used in place of (−)-**3** in the ring opening of cyclooctadiene monoxide, nonlinear effects were not observed with scalemic (*R,R*)-**2** (Figure S28). This indicates that a monometallic pathway is responsible for the fluoride ring opening of meso epoxides in the presence of **4**. Furthermore, the monometallic ring opening is unselective and slow compared to the bimetallic pathway observed with (−)-**3**. We hypothesize that **4**, a superior ligand and Lewis base compared to **3** on the basis of steric considerations and ring size,[51] outcompetes the meso epoxide as a neutral ligand to (salen)Co and prevents Lewis acid activation of the epoxide, which is required for the selective bimetallic pathway. The less sterically hindered terminal epoxides are sufficiently good ligands to (salen)Co to compete with cocatalyst **4** and thus undergo selective kinetic resolution in its presence.

Proposed Mechansim. On the basis of the data obtained thus far, we propose the mechanism depicted in Scheme 3. A salient feature of this catalytic cycle is that equilibrating fluoride-bridged dimers are the dominant contributors to the (salen)Co resting state. HFIP binding to (salen)CoF dimer **A** provides adduct **B**, and acyl transfer of the alkoxide with PhCOF provides bifluoride-containing dimer **C**. This species may bind to either matched or mismatched epoxide, providing $\mathbf{D_{mat}}$ and $\mathbf{D_{mismat}}$. Amidine association reveals the active monomeric components, which react in the rate-limiting step to generate ring-opened product. However, only the matched combination of (salen)Co and epoxide (**E**) productively engages the nucleophilic fluorine source **F**.

We propose that the active nucleophilic fluorinating agent is a metal bifluoride, **F**, on the basis of several considerations.[52] In the presence of a proton source such as HFIP, it is expected that the metal bifluoride would be thermodynamically favored.[53] Moreover, an inverse kinetic isotope effect $k_{HFIP}/k_{HFIP\text{-}d2} = 0.86$ is observed in the ring opening of **5**, indicating the involvement of a hydrogen bond in the rate-limiting step. The origin of such an inverse KIE could be attributed to F···HF bond breaking in the delivery of fluoride to the epoxide and is consistent with literature values;[54] however, other hydrogen-bonding interactions cannot be ruled out. Furthermore, presumed (salen)CoF and (salen)CrF species generated by us and by Haufe and co-workers, through metathesis of (salen)MCl with AgF in the absence of a proton source, provide inferior reactivity.[9] Kinetic considerations also disfavor a mechanism based on nucleophilic (salen)CoF: since the proposed resting state contains fluoride, such a scenario would provide zeroth-order dependence on PhCOF, not saturation behavior.

From the mechanism in Scheme 3, we derived a rate law using the equilibrium assumption and the simplification that the mass balance of Co is solely composed of dimeric complexes (see Supporting Information). Under the synthetically relevant conditions (high [PhCOF] and [HFIP]), this rate law is simplified to eq 7. It is important to note that the proposed mechanism disregards various off-cycle binding events, combinations of anionic and neutral ligands to (salen)Co that would provide less reactive complexes, and equilibria between monomeric species that likely contribute to the overall rate. Nevertheless, the derived rate law encompasses all of the key experimental observations, most notably: (1) first-order dependence on [**2**] and [**4**], (2) nonlinear effects obeying the ML_2 model, (3) saturation behavior in epoxide and PhCOF, (4) inhibition by mismatched epoxide, and (5) lack of inhibition by **7** at high [PhCOF] and [HFIP]. The complexities associated with HFIP dependence (vide supra) cannot be fully explained by eq 6; however, the zeroth-order dependence on [HFIP] observed under synthetically relevant concentrations is consistent with this proposal.

$$\text{rate} = \frac{(1/2)k_{cat}K_1K_2K_{mat}K_3[\text{Co}]_{tot}[\text{HFIP}][\text{PhCOF}][\mathbf{S}_{mat}][\mathbf{4}]}{\left([\mathbf{7}] + K_1[\text{HFIP}][\mathbf{7}] + K_1K_2[\text{HFIP}][\text{PhCOF}](1 + K_{mat}[\mathbf{S}_{mat}] + K_{mis}[\mathbf{S}_{mis}])\right)} \quad (6)$$

$$\text{rate} = \frac{(1/2)k_{cat}K_{mat}K_3[\text{Co}]_{tot}[\mathbf{S}_{mat}][\mathbf{4}]}{1 + K_{mat}[\mathbf{S}_{mat}] + K_{mis}[\mathbf{S}_{mis}]} \quad (7)$$

By fitting experimental data from kinetics experiments with (*R*)-**5** (eq 1) at varying concentrations of catalysts and substrates to eq 6, we obtained the constants shown in Scheme 3. An important consequence of this rate law is that inhibition by mismatched (*S*)-**5** may be quantified: we find that $K_{mat}/K_{mis} \approx 1$,

consistent with the conclusion that nonlinear effects in the kinetic resolution originate in bimetallic ring-opening, not selective binding of epoxide.

According to this proposed mechanism, the rate of the reaction would be affected by both the concentration of **F** and the rate constant of bimetallic ring opening. Thus, the influence of an amine cocatalyst on rate could be derived from its ability to both promote dissociation of dimer $\mathbf{D_{mat}}$ and to increase the nucleophilicity of bifluoride **F**. We hypothesize that amine binding confers greater nucleophilicity on a **2**·Nu species through the *trans* effect, as has been invoked in the use of Lewis basic additives for (salen)Mn-catalyzed epoxidations and **1**-catalyzed copolymerizations of epoxides and CO_2.[55] While free amine could play a role in acyl transfer,[56] the combination of (−)-**3** or **4** and benzoyl fluoride did not provide evidence of the acylammonium adduct by IR or NMR, indicating that the equilibrium for such a species is unfavorable.

Furthermore, the matched-mismatched effect on enantioselectivity observed in the ring opening of meso epoxides with (−)-**3** can also be explained by isothiourea binding to (salen)Co, which provides diasteriomeric complexes. Subtle conformational differences between (*R,R*)-**2**·FHF·(−)-**3** and (*S,S*)-**2**·FHF·(−)-**3** presumably result in different trajectories of attack and activation barriers ($\Delta\Delta G^{\ddagger}$) in the corresponding transition states. In accordance with this proposal, we observed moderate asymmetric induction for ring opening catalyzed by (−)-**3** in combination with an achiral variant of **2**.[7] Similarly, Katsuki and co-workers have demonstrated that chiral amine ligands induce detectable enantioselectivity for epoxidation in concert with achiral (salen)Mn catalysts.[57,58] As evidence of the great degree of order required in the transition state, Eyring analysis of the fluoride ring-opening of cyclooctadiene monoxide by the matched combination of catalysts provided a relatively large $\Delta S^{\ddagger}$ value (−32 eu) (see Supporting Information).

Synthetic Improvement with Linked Catalysts. As mentioned above, the use of dicarboxylate-linked catalyst **8**, prepared from a known suberate-linked salen ligand and $Co(OAc)_2$ in 87% yield on gram scale, afforded significant rate acceleration in the kinetic resolution of hexene oxide. Rate enhancement was also observed for other terminal epoxides (Table 2), including styrene oxides (entries 1−3) and *tert*-butyldimethylsilyl (TBS) glycidyl ether (entry 4). Furthermore, the substrate scope of the fluoride ring-opening kinetic resolutions could be expanded to include a secondary carbamate-containing epoxide (entry 5) and a propargylic epoxide (entry 6). In these cases, the substrates react sluggishly under standard reaction conditions with monomeric **2**. In contrast, reactions were complete in less than 4 h with 0.25−0.5 mol % catalyst **8**. Similar results were obtained for representative epoxides with a 30-min reaction time when 1.25 mol % **8** and 2 mol % **4** were employed (see Supporting Information). On the basis of the kinetics experiments described above, which showed saturation in PhCOF and zeroth-order dependence on HFIP, we also found that it is possible to use substoichiometric amounts of these reagents without adversely affecting rates or isolated yields.

Notably, the nitroimidazole-substituted fluorohydrin product **9** (Scheme 4) represents the "cold" version of the PET radiotracer fluoromisonidazole (F-MISO), which is used to detect hypoxia and predict cancer recurrence in living cells.[59] Currently, F-MISO is synthesized through fluoride displacement of a primary tosylate, and requires a deprotection step subsequent to fluorination.[60] With 1.25 mol % **8**, fluoride ring opening was achieved within 5 min, providing **9** directly in 40% isolated yield and 93% ee from racemic epoxide.[61] Benzoyl fluoride is manufactured from benzoyl chloride and KF by a Halex process, which should be amenable to the synthesis of PhCO^{18}F.[62] While our own catalytic method has not yet been optimized to meet the stringent requirements of radiochemical synthesis, the synthesis of **9** showcases the functional-group tolerance and convenient reaction rates afforded by **8**.

Improved rates, enantioselectivities, and substrate scope can also be achieved for the desymmetrization of meso epoxides when **8** is used in conjunction with amidine cocatalyst **4** (Table 3).[63]

Table 2. Kinetic Resolution of Terminal Epoxides Catalyzed by 8[a]

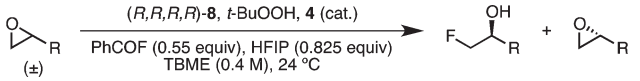

entry	product	8 (mol %)	time (h)	yield (%)[b]	ee (%)[c]	s[d]
1	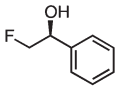	0.125	3.5	42	98	211
2	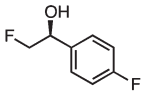	0.125	2	42	98	211
3	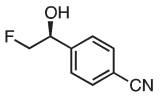	0.125	2	43	99	449
4	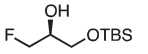	0.25	4	44	96	112
5	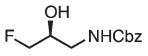	0.25	3	44	90	40
6	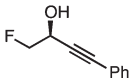	0.5	2	45	98	245

[a] 1.6 equiv of **4** and 2 equiv of *t*-BuOOH were used relative to **8**. In entries 1−3, 0.45 equiv of PhCOF was used relative to epoxide. [b] Isolated yields for 1−8 mmol scale; theoretical maximum is 50% yield. [c] Determined using chiral GC or HPLC analysis on commercial columns. [d] *s* represents a lower bound for the selectivity factor calculated from the isolated yield (C) and ee of product (ee): $s = \ln[1 - C(1 + \text{ee})]/\ln[1 - C(1 - \text{ee})]$.

Scheme 4. Synthesis of F-MISO (9)

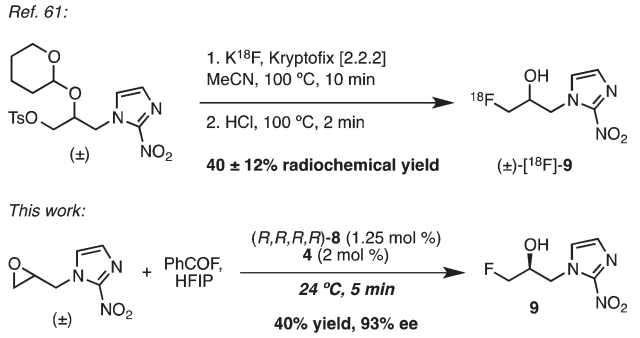

Table 3. Desymmetrization of Meso Epoxides Catalyzed by 8[a]

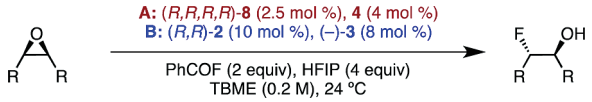

entry	product	conditions	time (h)	yield (%)[b]	ee (%)[c]
1		**A**[d]	18	79	97
		B[d]	72	77	85
2	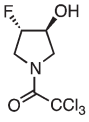	**A**[e]	3	89	98
		B[f]	120	84	80
3	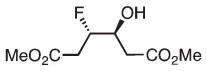	**A**[g]	96	82	87
		B	120	(30)	84

[a] See ref 7 for experimental details regarding conditions B. [b] Isolated yields for 0.5−2 mmol scale; conversions determined by GC using 1-decene as an internal standard are in parentheses. [c] Determined using chiral GC or HPLC analysis on commercial columns. [d] Reaction conducted in Et_2O. [e] Reaction conducted with 1.25 mol % **8**, 2 mol % **4**. [f] Reaction conducted in *t*-AmOH. [g] Reaction conducted with 5 mol % **8**, 8 mol % **4**.

Direct comparisons in the opening of cyclopentene oxide (entry 1) and a protected pyrrolidine-derived epoxide (entry 2) demonstrate the significance of the synthetic improvement. Furthermore, an acyclic meso epoxide, which underwent minimal ring opening under catalysis by **2**, provided fluorohydrin product in good yield and ee (entry 3). The success of the linked-catalyst strategy suggests that other well-developed dimeric and oligomeric catalysts could be used to further improve the rates, enantioselectivities, and substrate scope of the fluorinations.[14]

CONCLUSION

The multicomponent nature of the cooperative cocatalytic fluorination, which employs benzoyl fluoride and HFIP as a latent HF source, renders elucidation of the catalytic mechanism a challenging endeavor. However, mechanistic insight has been gained through a combination of experiments aimed at identifying the active fluorinating reagent and composition of the rate-limiting step. In particular, substituent effects in the fluoride ring opening of *para*-substituted styrene oxides have established that ring opening is rate limiting. A bimetallic mechanism for this step is proposed based on nonlinear effects studies with monomeric (salen)Co catalysts and experiments using a linked catalyst. In light of the above experiments and the established mechanism for (salen)Co-catalyzed epoxide ring opening with other nucleophiles, observation of a first-order dependence on [(salen)Co] was unexpected. Our study highlights that, in the absence of structural information about the resting state, observation of a first-order dependence on [catalyst] is not sufficient to establish that only one catalyst species participates in the rate-determining step. As such, a resting state composed of fluoride-bridged dimers likely accounts for the discrepancy between the kinetic studies and the Hammett correlation and nonlinear effects presented in this paper. With this insight, we were able to improve the protocols for enantioselective fluoride ring opening of terminal and meso epoxides. Use of a linked (salen)Co catalyst afforded significantly elevated rates, expanded substrate scope, and high enantioselectivity in the synthesis of β-fluoro alcohols, which represent valuable fluorinated building blocks for chemical synthesis.

While many of the subtle factors governing cooperative catalysis in this system have yet to be fully unraveled, evidence for the role of the amine cocatalyst has been obtained. To this end, we have introduced a model for studying nonlinear effects in reactions that involve two chiral catalysts. Furthermore, spectroscopic studies have revealed that the amine cocatalysts serve as ligands for (salen)Co. On the basis of these data, we propose that the role of the amine is to facilitate dissociation of a (salen)Co dimer to its active monomeric components. Additional contributions to the pronounced matched/mismatched effects may derive from the ability of the cocatalysts to influence the lability of the axial bifluoride ligand and the conformation of the salen backbone. We anticipate that the mechanistic understanding gained in these studies will allow us to design asymmetric nucleophilic fluorination reactions with other electrophilic partners. Most promising in this regard is the discovery that a chiral, organic-soluble metal fluoride can be accessed under mild catalytic conditions and is an effective fluoride delivery agent.

ASSOCIATED CONTENT

Supporting Information. Experimental procedures and spectroscopic data for all new compounds; derivations of eqs 4−6; additional nonlinear effects, kinetic data, and Eyring analysis. This material is available free of charge via the Internet at http://pubs.acs.org.

AUTHOR INFORMATION

Corresponding Author
agdoyle@princeton.edu

ACKNOWLEDGMENT

Financial support was provided by Princeton University, kind gifts from Eli Lilly and Sanofi-Aventis (A.G.D.), the donors of the American Chemical Society Petroleum Research Fund, and Bristol-Myers Squibb (fellowhip to J.A.K.). This material is based upon work supported by the National Science Foundation Graduate Research Fellowship under Grant No. DGE-0646086 (J.A.K.). The authors thank Dr. Stephan Zuend for helpful discussions.

REFERENCES

(1) (a) Banks, R. E., Smart, B. E., Tatlow, J. C., Eds. *Organofluorine Chemistry: Principles and Commercial Applications*; Plenum Press: New York, 1994. For recent reviews of the role of fluorine in medicinal chemistry, see: (b) Müller, K.; Faeh, C.; Diederich, F. *Science* **2007**, *317*, 1881–1886. (c) Hagmann, W. K. *J. Med. Chem.* **2008**, *51*, 4359–4369. (d) Purser, S.; Moore, P. R.; Swallow, S.; Gouverneur, V. *Chem. Soc. Rev.* **2008**, *37*, 320–330.

(2) O'Hagan, D. *Chem. Soc. Rev.* **2008**, *37*, 308–319.

(3) Furuya, T.; Kuttruff, C. A.; Ritter, T. *Curr. Opin. Drug Discovery Dev.* **2008**, *11*, 803–819 and references therein.

(4) For a review, see: Ametamey, S. M.; Honer, M.; Schubiger, P. A. *Chem. Rev.* **2008**, *108*, 1501–1516.

(5) For recent reviews of asymmetric catalytic C−F bond formation, see: (a) Ma, J.-A.; Cahard, D. *Chem. Rev.* **2008**, *108*, PR1–PR43. (b) Lectard, S.; Hamashima, Y.; Sodeoka, M. *Adv. Synth. Catal.* **2010**, *352*, 2708–2732.

(6) Clark, J. H. *Chem. Rev.* **1980**, *80*, 429–452.
(7) Kalow, J. A.; Doyle, A. G. *J. Am. Chem. Soc.* **2010**, *132*, 3268–3269.
(8) Katcher, M. H.; Doyle, A. G. *J. Am. Chem. Soc.* **2010**, *132*, 17402–17404. This report describes the palladium-catalyzed asymmetric synthesis of allylic fluorides through S_N2 attack of fluoride on a π-allyl intermediate.
(9) (a) Bruns, S.; Haufe, G. *J. Fluorine Chem.* **2000**, *104*, 247–254. (b) Haufe, G.; Bruns, S. *Adv. Synth. Catal.* **2002**, *344*, 165–171.
(10) Olah, G. A.; Welch, J. T.; Vankar, Y. D.; Nojima, M.; Kerekes, I.; Olah, J. A. *J. Org. Chem.* **1979**, *44*, 3872–3881.
(11) Jacobsen, E. N. *Acc. Chem. Res.* **2000**, *33*, 421–431.
(12) (a) Hansen, K. B.; Leighton, J. L.; Jacobsen, E. N. *J. Am. Chem. Soc.* **1996**, *118*, 10924–10925. (b) Konsler, R. G.; Karl, J.; Jacobsen, E. N. *J. Am. Chem. Soc.* **1998**, *120*, 10780–10781.
(13) Nielsen, L. P. C.; Stevenson, C. P.; Blackmond, D. G.; Jacobsen, E. N. *J. Am. Chem. Soc.* **2004**, *126*, 1360–1362.
(14) A number of oligomeric analogues of **2** have been discovered that serve as excellent catalysts in ring-opening reactions by favoring cooperative bimetallic interactions. For reviews, see: (a) Zhu, X.; Venkatasubbaiah, K.; Weck, M.; Jones, C. W. *ChemCatChem* **2010**, *2*, 1252–1259. (b) Haak, R. M.; Wezenberg, S. J.; Kleij, A. W. *Chem. Commun.* **2010**, *46*, 2713–2723.
(15) Blackmond, D. G. *Angew. Chem., Int. Ed.* **2005**, *44*, 4302–4320.
(16) Unlike ^{1}H NMR, ^{19}F NMR does not suffer significant peak broadening in the presence of (salen)Co(III). Furthermore, ^{19}F NMR allowed the reaction to be performed in TBME, which is not readily available as TBME-d_{12}.
(17) Oxidation occurs readily in the presence of air and acid: Jacobsen, E. N.; Kakiuchi, F.; Konsler, R. G.; Larrow, J. F.; Tokunaga, M. *Tetrahedron Lett.* **1997**, *38*, 773–776. Additionally, (1) reactions conducted under a N_2 atmosphere exhibited an extended induction period, and (2) product added to the reactions did not affect the reaction rates, eliminating the possibility of product autocatalysis. See Supporting Information.
(18) However, **4** decomposes over time to the catalytically inactive lactam **4′** (shown below) when exposed to ambient moisture. Therefore, commercial **4** should be distilled from CaH_2 and stored over activated 3 Å molecular sieves: Shaw, T. W.; Kalow, J. A.; Doyle, A. G. *Org. Synth.* **2012**, *89*, 9–18. Chiral isothiourea **3** does not exhibit hydrolysis under ambient conditions.

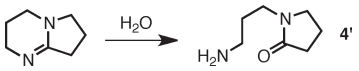

(19) We found that benzoyl fluoride stored under air undergoes slow hydrolysis to provide small quantities of benzoic acid; the presence of this impurity reduced reaction rates. Therefore, in these experiments, we employed purified benzoyl fluoride. For synthetic applications, however, this precaution is not necessary. See Supporting Information for details.
(20) Alternatively, unproductive H-bonding interactions between HFIP and various Lewis basic components of the reaction could account for this rate inhibition. HFIP is well known to have unique properties as a solvent and additive: Shuklov, I. A.; Dobrovina, N. V.; Börner, A. *Synthesis* **2007**, 2925–2943.
(21) Hammett, L. P. *J. Am. Chem. Soc.* **1937**, *59*, 96–136.
(22) All of the substrates employed react selectively under these conditions, confirming that unselective background reaction is not responsible for the differences in rate. Selectivity factor *s* is calculated here from the conversion (*C*) and ee (*ee*) of epoxide: $s = \ln[(1 - C)(1 - ee)]/\ln[(1 - C)(1 + ee)]$. For a discussion of kinetic resolutions, see: Keith, J. M.; Larrow, J. F.; Jacobsen, E. N. *Adv. Synth. Catal.* **2001**, *343*, 5–26.
(23) Hammet constants σ_m were obtained from: Speight, J. G. In *Lange's Handbook of Chemistry*, 16th ed.; McGraw-Hill: New York, 2005; Chapter 2.19, pp 2.702−2.709. For Hammett correlations of the rate data using other σ constants, see the Supporting Information.
(24) It is expected that ring opening at the terminal position of the styrene oxides would be influenced primarily by inductive effects, and σ_m is frequently used as a measure of inductive effects in substituted benzene rings even if the substituent is not *meta* to the reactive center. See: (a) Wheeler, S. E.; Houk, K. N. *J. Am. Chem. Soc.* **2008**, *130*, 10854–10855. (b) Wheeler, S. E.; McNeil, A. J.; Müller, P.; Swager, T. M.; Houk, K. N. *J. Am. Chem. Soc.* **2010**, *132*, 3304–3311.
(25) Pedragosa-Moreau, S.; Morisseau, C.; Zylber, J.; Archelas, A.; Baratti, J.; Furstoss, R. *J. Org. Chem.* **1996**, *61*, 7402–7407.
(26) (a) Laird, R. M.; Parker, R. E. *J. Am. Chem. Soc.* **1961**, *83*, 4277–4281. (b) Blumenstein, J. J.; Ukachukwu, V. C.; Mohan, R. S.; Whalen, D. L. *J. Org. Chem.* **1993**, *58*, 924–932. In contrast, ring-opening reactions that follow a S_N1-like pathway favor internal opening and have large negative ρ values that correlate to σ_p.
(27) Ring opening by fluoride is irreversible under the reaction conditions; thus, the ring-opening step (in which a prochiral epoxide is transformed into chiral fluorohydrin, or in which one enantiomer of racemic epoxide reacts selectively) is inherently the enantiodetermining step.
(28) Since the ee of the product changes over the course of kinetic resolutions, a direct comparison of $ee_{product}$ vs ee_{cat} is not meaningful. See: Johnson, D. W.; Singleton, D. A *J. Am. Chem. Soc.* **1999**, *121*, 9307–9312.
(29) Blackmond, D. G. *J. Am. Chem. Soc.* **2001**, *123*, 545–553.
(30) Blackmond, D. G. *Acc. Chem. Res.* **2000**, *33*, 402–411.
(31) For examples involving negative nonlinear effects and rate amplification, see: (a) Kina, A.; Iwamura, H.; Hayashi, T. *J. Am. Chem. Soc.* **2006**, *128*, 3904–3905. (b) Duan, W.-L.; Iwamura, H.; Shintani, R.; Hayashi, T. *J. Am. Chem. Soc.* **2007**, *129*, 2130–2138. For an example involving positive nonlinear effects and rate suppression, see: (c) Yamagiwa, N.; Qin, H.; Matsunaga, S.; Shibasaki, M. *J. Am. Chem. Soc.* **2005**, *127*, 13419–13427.
(32) Girard, C.; Kagan, H. B. *Angew. Chem., Int. Ed.* **1998**, *37*, 2922–2959.
(33) *K* is a property of the catalyst and should be independent of the substrate (for an exception, see Kitamura, M.; Suga, S.; Oka, H.; Noyori, R. *J. Am. Chem. Soc.* **1998**, *120*, 9800–9809), but *g* is dependent on substrate.
(34) For a schematic explanation, see Scheme S1 (Supporting Information).
(35) For an example in the Sharpless asymmetric epoxidation, see: Puchot, C.; Samuel, O.; Dunach, E.; Zhao, S.; Agami, C.; Kagan, H. B. *J. Am. Chem. Soc.* **1986**, *108*, 2353–2357.
(36) Nielsen, L. P. C. Ph.D. Thesis, Harvard University, 2006.
(37) (a) Wu, M. H.; Hansen, K. B.; Jacobsen, E. N. *Angew. Chem., Int. Ed.* **1999**, *38*, 2012–2014. (b) Nakano, K.; Hashimoto, S.; Nozaki, K. *Chem. Sci.* **2010**, *1*, 369–373. In the latter case, a heterochiral adipate-bridged catalyst was found to be optimal.
(38) **8** does not undergo aerobic oxidation readily at these catalyst loadings under the standard reaction conditions; *t*-BuOOH promotes immediate oxidation without detrimental effects on yield or ee.
(39) An acetylated, C_1-symmetric monomeric catalyst promotes reaction more slowly than **2** does, suggesting that the rate acceleration is not due to the electronic differences in the dicarboxylate-linked **8**.
(40) The fluoride ring opening of (±)-hexene oxide catalyzed by **2** also exhibits a first-order dependence on [**2**], consistent with the kinetic data obtained using (*R*)-**5**; see Supporting Information.
(41) For representative examples, see: (a) Ng Cheong Chan, Y.; Osborn, J. A. *J. Am. Chem. Soc.* **1990**, *112*, 9400–9401. (b) Mccleland, B. W.; Nugent, W. A.; Finn, M. G. *J. Org. Chem.* **1998**, *63*, 6656–6666. (c) Bandini, M.; Cozzi, P. G.; Umani-Ronchi, A. *Tetrahedron* **2001**, *57*, 835–843. (d) Rosner, T.; Le Bars, J.; Pfaltz, A.; Blackmond, D. G. *J. Am. Chem. Soc.* **2001**, *123*, 1848–1855. (e) ref 31a. In (b) and (c), resting-state tetramers and an active dimeric catalyst are proposed.
(42) A conceptually analogous scenario, for an enzymatic reaction that exhibits overall first-order kinetics but is experimentally determined to be bimolecular, has been described: Baker, G. M.; Weng, L. *J. Theor. Biol.* **1992**, *158*, 221–229.
(43) For reviews, see: (a) Murphy, E. F.; Murugavel, R.; Roesky, H. W. *Chem. Rev.* **1997**, *97*, 3425–3468. (b) Tramšek, M.; Goreshnik, E.; Lozinšek, M.; Žemva, B. *J. Fluorine Chem.* **2009**, *130*, 1093–1098. For a recent example of a crystallographically characterized $[Co^{II}(\mu\text{-}F)]_2$ complex, see: (c) Dugan, T. R.; Sun, X.; Rybak-Akimova, E. V.;

Olatunji-Ojo, O.; Cundari, T. R.; Holland, P. L. *J. Am. Chem. Soc.* **2011**, *133*, 12418–12421.

(44) For an achiral (salen)Co coordination polymer of the form $[(salen)Co(OMe)(HOMe)_2]_n$ that has been isolated and analyzed by X-ray diffraction, see: Ajiro, H.; Peretti, K. L.; Lobkovsky, E. B.; Coates, G. W. *Dalton Trans.* **2009**, 8828–8830.

(45) ^{19}F NMR resonances have not been observed in spectra of the active complex; however, this behavior is expected on the basis of fast relaxation in a Co(III)-bound fluorine nucleus.

(46) Epoxides and THF appear to promote dissociation of $[\mathbf{1}\cdot\mu\text{-}N_3]_n$ (see ref 12a).

(47) X-ray structures of (salen)Co species crystallized in the presence of amine ligands provide further support for a (salen)Co·amine adduct: (a) Marzilli, L. G.; Summers, M. F.; Bresciani-Pahor, N.; Zangrando, E.; Charland, J. P.; Randaccio, L. *J. Am. Chem. Soc.* **1985**, *107*, 6880–6888. (b) Zhang, Y.; Ruan, W.; Zhao, X.; Wang, H.; Zhu, Z. *Polyhedron* **2003**, *22*, 1535–1545. (c) Thomas, R. M.; Widger, P. C. B.; Ahmed, S. M.; Jeske, R. C.; Hirahata, W.; Lobkovsky, E. B.; Coates, G. W. *J. Am. Chem. Soc.* **2010**, *132*, 16520–16525.

(48) Kemper et al. concluded that nucleophilic **2**·Cl was five-coordinate on the basis of NMR experiments and computational modeling: (a) Kemper, S.; Hrobárik, P.; Kaupp, M.; Schlörer, N. E. *J. Am. Chem. Soc.* **2009**, *131*, 4172–4173. ; however, **2**·Cl may not be a respresentative catalytic species, as ring opening with chloride is only moderately selective: (b) Thakur, S. S.; Li, W.-J.; Shin, C.-K.; Kim, G.-J. *Chirality* **2006**, *18*, 37–43. Furthermore, detailed kinetic studies and computational analysis of the HKR (see refs 13 and 36) reveal that the nucelophilic **2**·OH species is six-coordinate, with H_2O as the neutral axial ligand.

(49) For other examples of chiral Lewis acid−chiral amine cocatalysis that display a matched/mismatched effect on rate and enantioselectivity, see: (a) Kobayashi, S.; Kawamura, M. *J. Am. Chem. Soc.* **1998**, *120*, 5840–5841. (b) Ding, K.; Ishii, A.; Mikami, K. *Angew. Chem., Int. Ed.* **1999**, *38*, 497–501. (c) Gou, S.; Chen, X.; Xiong, Y.; Feng, X. *J. Org. Chem.* **2006**, *71*, 5732–5736. (d) Mashiko, T.; Kumagai, N.; Shibasaki, M. *J. Am. Chem. Soc.* **2009**, *131*, 14990–14999.

(50) Significant nonlinear effects have been observed for mixtures of pseudoenantiomeric or diastereomeric catalysts, and in some cases have been used to enhance mechanistic understanding: (a) Zhang, S. Y.; Girard, C.; Kagan, H. B. *Tetrahedron: Asymmetry* **1995**, *6*, 2637–2640. (b) Blackmond, D. G.; Rosner, T.; Neugebauer, T.; Reetz, M. T. *Angew. Chem., Int. Ed.* **1999**, *38*, 2196–2199. (c) Bolm, C.; Muñiz, K.; Hildebrand, J. P. *Org. Lett.* **1999**, *1*, 491–493.

(51) (a) Birman, V. B.; Li, X.; Han, Z. *Org. Lett.* **2007**, *9*, 37–40. (b) Baidya, M.; Mayr, H. *Chem. Commun.* **2008**, 1792–1794. (c) Maji, B.; Joanesse, C.; Nigst, T. A.; Smith, A. D.; Mayr, H. *J. Org. Chem.* **2011**, *76*, 5104–5112.

(52) Transition-metal bifluorides have been characterized by NMR, IR, and X-ray and neutron diffraction, but have not been used extensively as nucleophilic fluorine sources. For representative examples, see: (a) Murphy, V. J.; Hascall, T.; Chen, J. Y.; Parkin, G. *J. Am. Chem. Soc.* **1996**, *118*, 7428–7429. (b) Murphy, V. J.; Rabinovich, D.; Hascall, T.; Klooster, W. T.; Koetzle, T. F.; Parkin, G. *J. Am. Chem. Soc.* **1998**, *120*, 4372–4387. (c) Jasim, N. A.; Perutz, R. N. *J. Am. Chem. Soc.* **2000**, *122*, 8685–8693. (d) Roe, D. C.; Marshall, W. J.; Davidson, F.; Soper, P. D.; Grushin, V. V. *Organometallics* **2000**, *19*, 4575–4582. For an example of a bifluoride-bridged Nb dimer, see: (e) Roesky, H. W.; Sotoodeh, M.; Xu, Y.; Schrumpf, F.; Noltemeyer, M. *Z. Anorg. Allg. Chem.* **1990**, *580*, 131–138.

(53) (a) Fraser, S. L.; Antipin, M. Y.; Khroustalyov, V. N.; Grushin, V. V. *J. Am. Chem. Soc.* **1997**, *119*, 4769–4770. (b) Pilon, M. C.; Grushin, V. V. *Organometallics* **1998**, *17*, 1774–1781.

(54) (a) Basolo, F.; Matoush, W. R.; Pearson, R. G. *J. Am. Chem. Soc.* **1956**, *78*, 4883–4886. (b) Kresge, A. J.; Chiang, Y. *J. Phys. Chem.* **1973**, *77*, 822–825.

(55) (a) Deng, L.; Jacobsen, E. N. *J. Org. Chem.* **1992**, *57*, 4320–4323. (b) Darensbourg, D. J.; Mackiewicz, R. M. *J. Am. Chem. Soc.* **2005**, *127*, 14026–14038.

(56) For amine- and NHC-catalyzed reactions using acid fluorides for the activation of silicon-containing substrates, an acyl transfer mechanism may be relevant: (a) Bappert, E.; Muller, P.; Fu, G. C. *Chem. Commun.* **2006**, 2604–2606. (b) Poisson, T.; Dalla, V.; Marsais, F.; Dupas, G.; Oudeyer, S.; Levacher, V. *Angew. Chem., Int. Ed.* **2007**, *46*, 7090–7093. (c) Ryan, S. J.; Candish, L.; Lupton, D. W. *J. Am. Chem. Soc.* **2011**, *133*, 4694–4697.

(57) (a) Hashihayata, T.; Ito, Y.; Katsuki, T. *Tetrahedron.* **1997**, *53*, 9541–9552. (b) Miura, K.; Katsuki, T. *Synlett.* **1999**, 783–785. and references therein. Additionally, Liao and List have demonstrated that chiral phosphate counterions can induce asymmetry in achiral (salen)Mn-catalyzed epoxidations, possibly through a "frustrated" ion pair: Liao, S.; List, B. *Angew. Chem., Int. Ed.* **2010**, *49*, 628–631.

(58) Additionally, Fuiji and coworkers have observed that achiral axial ligands to (salen)Mn(IV) can amplify the stepped conformation of the chiral salen backbone: Kurahashi, T.; Hada, M.; Fujii, H. *J. Am. Chem. Soc.* **2009**, *131*, 12394–12405.

(59) Couturier, O.; Luxen, A.; Chatal, J.-F.; Vuillez, J.-P.; Rigo, P.; Hustinx, R. *Eur. J. Nucl. Med. Mol. Imaging* **2004**, *31*, 1182–1206.

(60) (a) Kämäräinen, E.-L.; Kyllönen, T.; Nihtilä, O.; Björk, H.; Solin, O. *J. Labelled Compd. Radiopharm.* **2004**, *47*, 37–45. A recent patent discloses a strategy for direct fluorination of the epoxide using $K^{18}F$/Kryptofix in the presence of *t*-butanol or *t*-amyl alcohol: (b) Moon, D. H.; Chi, D. Y.; Kim, D. W.; Oh, S. J.; Ryu, J. Patent WO 2006/065038 A1, June 22, 2006.

(61) To the best of our knowledge, differences between (*R*)- and (*S*)-^{18}F-MISO have not been reported: Nieto, E.; Alajarín, R.; Álvarez-Builla, J.; Larrañaga, I.; Gorospe, E.; Pozo, M. *Synthesis* **2010**, 3700. Nevertheless, use of (±)-**8** as a catalyst for the racemic synthesis of **9** would be more direct than the current radiosynthetic protocol. The THP-protected precursor for this route is made in four steps whereas the epoxide precursor in Scheme 4 is accessible in two steps from epichlorohydrin and 2-nitroimidazole.

(62) (a) Olah, G. A.; Kuhn, S. J.; Dupont, J. A.; Emmons, W. D. *Org. Synth.* **1965**, *45*, 3. and references therein. (b) Troy Ryba, Sigma Aldrich. Personal communication, 2011.

(63) With (*R*,*R*,*R*,*R*)-**8**, cocatalyst (−)-**3** provided lower rates than the **4**/**8** combination with no significant change in ee; it is likely that the monometallic pathway responsible for low rates and ee's with the combination of (*R*,*R*)-**2** and **4** is disfavored when the (salen)Co are linked.